Multibody Syst Dyn (2012) 28:109–124
DOI 10.1007/s11044-011-9284-5

# A simple approach to estimate muscle forces and orthosis actuation in powered assisted walking of spinal cord-injured subjects

**J. Alonso · F. Romero · R. Pàmies-Vilà · U. Lugrís · J.M. Font-Llagunes**

Received: 11 May 2011 / Accepted: 2 November 2011 / Published online: 3 January 2012


**Abstract** Simulation of walking in individuals with incomplete spinal cord injuries (SCI) wearing an active orthosis is a challenging problem from both the analytical and the computational points of view, due to the redundant nature of the simultaneous actuation of the two systems. The objective of this work is to quantify the contributions of muscles and active orthosis to the net joint torques, so as to assist the design of active orthoses for SCI. The functional innervated muscles of SCI patients were modeled as Hill-type actuators, while the idle muscles were represented by elastic and dissipative elements. The orthosis was included as a set of external torques added to the ankles, knees, and hips to obtain net joint torque patterns similar to those of normal unassisted walking. The muscle-orthosis redundant actuator problem was solved through a physiological static optimization approach, for which several cost functions and various sets of innervated muscles were compared.

**Keywords** Spinal cord injuries · Active orthoses · Musculoskeletal modeling · Optimization · Inverse dynamics

J. Alonso (✉) · F. Romero
Universidad de Extremadura, Avda. de Elvas s/n, 06006 Badajoz, Spain
e-mail: fjas@unex.es

R. Pàmies-Vilà · J.M. Font-Llagunes
Universidad Politécnica de Cataluña, Av. Diagonal 647, 08028 Barcelona, Spain

R. Pàmies-Vilà
e-mail: rosa.pamies@upc.edu

J.M. Font-Llagunes
e-mail: josep.m.font@upc.edu

U. Lugrís
Universidad de La Coruña, Mendizábal s/n, 15403 Ferrol, Spain
e-mail: ulugris@udc.es

## 1 Introduction

Spinal cord injuries cause paralysis of the lower limb extremities as they break the connections from the central nervous system to the muscles of the lower body. Incomplete spinal cord-injured (SCI) subjects can perform a low-speed, high-cost pathological gait by using walking aids such as crutches, canes, or parallel bars. The energy cost and aesthetics of this gait can be improved by means of active orthoses, which require external actuation mechanisms to control the motion of the leg joints during the stance and swing phases of gait. To guide the development of active orthoses for SCI subjects, it is necessary to understand how the patient musculoskeletal actuation interacts with powered assistance to obtain a normal gait pattern. Considerable effort has been focused on the design and application of passive and active orthoses to assist standing and walking of SCI individuals. Nevertheless, few studies [1–7] examine the moment joint patterns of combined patient-orthosis systems.

The first controllable active orthosis that can be found is a patent from 1942 of a hydraulically-actuated device for adding power at the hip and knee joints [8]. The first active exoskeletons were developed at the University of Belgrade in the 1960s and 1970s to aid people with paraplegia resulting from spinal cord injury [8, 9]. These early devices were limited to predefined motions and had limited success. However, new laboratory and commercially available rehabilitation devices and active orthoses designs have emerged in the last 10 years. The proposed active orthotic devices add or dissipate power at their joints and/or release energy stored in springs during appropriate phases of gait [10]. These systems use in general a predefined motion pattern or moment joint pattern, qualitative and heuristic rules, classical control techniques, or EMG-based control, but ignore the interaction between the human musculoskeletal system and the active orthosis. Moreover, the number of studies testing these systems on handicapped subjects is paradoxically low when compared with the studies on able-bodied subjects wearing the orthosis.

For example, the "Locomat" uses a predefined motion strategy to train muscles and nerve pathways for patients with locomotion impairment [11]. The "RoboKnee" is a powered knee brace developed by MIT that functions in parallel to the wearer's knee and transfers load to the wearer's ankle [12]. "HAL" is an orthosis developed by the University of Tsukuba in Japan that is connected to the patient's thighs and shanks, and provides a motion to its legs that is a function of the measured EMG signals [13, 14]. The MIT Biomechatronics Lab developed a powered ankle-foot orthosis to assist drop-foot gait [15]: It consists of a modified passive ankle-foot orthosis with the addition of a series elastic actuator (SEA) to allow for variation in the impedance of dorsiflexion/plantar flexion motion of the ankle; the control of this device is based on ground contact force measurement and angle position data. Other approaches include the excitation of SCI muscles through the application of functional neuromuscular stimulation (FNS) [6, 16]. However, excitation in FNS only systems can lead to instability, poor control, and limited walking distances due to muscle fatigue [6, 16].

To assist the proper design of active orthoses for incomplete SCI, it is necessary to quantify the simultaneous contributions of muscles and active orthosis to the net joint torques of the human-orthosis system. Simulation of walking in individuals with incomplete SCI wearing an active orthosis is a challenging problem from both the analytical and the computational points of view, due to the redundant nature of the simultaneous actuation of the two systems. In this work, the functional innervated muscles of SCI patients were modeled as Hill-type actuators, while the idle muscles were represented by elastic and dissipative elements that increment the passive moments of the inactive joints.

The orthosis was included as a set of external torques added to the ankles, knees and hips to obtain net joint torque patterns similar to those of normal unassisted walking [2–4]. Kao et al. [2–4] suggest that able-bodied subjects aim for similar joint moment patterns

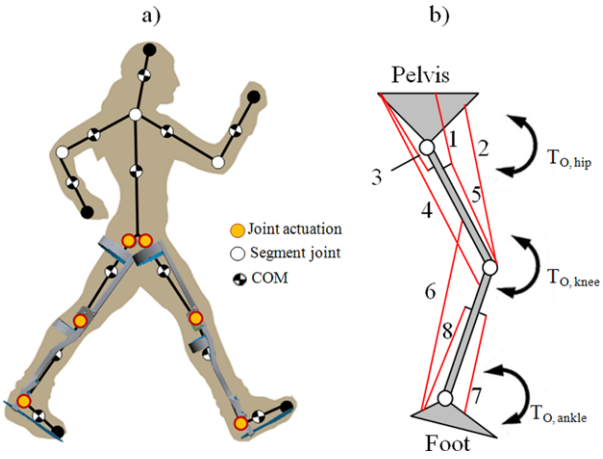


**Fig. 1** (**a**) Planar biomechanical model of the human-orthosis system. (**b**) Muscle groups: *1*—iliopsoas, *2*—rectus femoris, *3*—glutei, *4*—hamstrings, *5*—vasti, *6*—gastrocnemius, *7*—tibialis anterior, *8*—soleus

when walking with and without robotic assistance rather than similar kinematic patterns. The fundamental hypothesis of this work is that the combined actuation of the musculoskeletal system of the SCI subject and the active orthosis produce net joint moment patterns similar to those of normal unassisted walking. The muscle-orthosis redundant actuator problem was solved through a physiological static optimization approach, for which several cost functions and various sets of innervated muscles were compared.

## 2 Biomechanical model

The biomechanical model used has 14 degrees of freedom. It consists of 12 rigid bodies linked with revolute joints (Fig. 1), and it is constrained to move in the sagittal plane. Each rigid body is characterized by mass, length, moment of inertia about the center of mass and distance from the center of mass to the proximal joint.

The equations of motion can be written as

$$\mathbf{M}\ddot{\mathbf{q}} + \mathbf{\Phi}_{\mathbf{q}}^{T}\boldsymbol{\lambda} = \mathbf{Q} \tag{1}$$

where $\mathbf{M}$ is the system mass matrix, $\mathbf{\Phi}_{\mathbf{q}}$ is the Jacobian matrix of the constraint equations, $\ddot{\mathbf{q}}$ is the acceleration vector, $\mathbf{Q}$ is the generalized force vector, and $\boldsymbol{\lambda}$ are the Lagrange multipliers. Using kinematic and anthropometric data in (1), the net joint reaction forces and net driver (human-orthosis actuation) moments during a physical activity or motion and the ground reaction forces can be estimated. Nevertheless, it is well known that this procedure is highly error-prone because in the double stance phase there is no unique solution for the ground reaction forces at each foot. Moreover, it requires velocity and acceleration information, which is frequently obtained by numerical differentiation of position information acquired in standard gait analysis labs: This procedure amplifies noise and has been shown to lead to erroneous estimations of joint moments. Consequently, most studies use measured ground reaction forces along with kinematic and anthropometric data to estimate net joint reaction forces and net driver moments. In order to quantify the simultaneous contributions of muscles and active orthosis to the net joint torques of the human-orthosis system, eight muscle groups and three external torques added to the ankles, knees, and hips were considered in this analysis (shown in Fig. 1b). The proposed external actuation is an active hip-knee-ankle-foot orthosis (A-HKAFO) to provide hip, knee, and ankle joint moments to assist the pathological gait of SCI subjects.

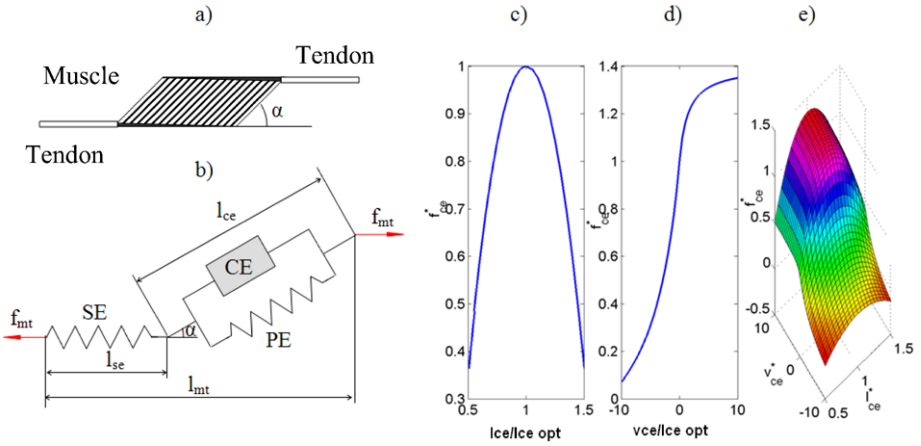


**Fig. 2** Muscle model for innervated muscles. (**a**) Conceptual scheme, (**b**) Hill model [17], (**c**) Normalized force–length relation model, (**d**) Normalized force–velocity relation model, and (**e**) Force–length–velocity model

## 2.1 Muscle model: innervated muscles

The functional innervated muscles of SCI patients were modeled as Hill-type actuators. Zajac [17] presented in 1989 the widely known Hill-type muscle-tendon model [18], which is shown in Figs. 2a and 2b. The model consists of a contractile element (CE) that generates the force, a nonlinear parallel elastic element (PE), representing the stiffness of the structures in parallel with muscle fibers, and a nonlinear series elastic (SE) element that represents the stiffness of the tendon which is serially attached to the muscle and completes the musculotendon unit.

The two differential equations that govern the muscle dynamics are:

$$\dot{a} = h(u, a) \tag{2}$$

$$\dot{f}_{mt} = g\left(l_{mt}, \dot{l}_{mt}, a, f_{mt}\right) \tag{3}$$

The first equation is the activation dynamics equation that relates muscle excitation $u$ from the central nervous system (CNS) and muscle activation $a$. Equation (3) defines the force-generation properties as a function of force–fiber length $l_{mt}$ and force–fiber velocity $\dot{l}_{mt}$ relationships. Activation and deactivation dynamics represent a delay with respect to the neural excitation that strongly influences the neural control strategy used and may be the governing muscle property that limits performance. Nevertheless, in this work, the activation dynamics was not considered as the presented optimization approach does not use neural excitations.

The force generated by the CE, $f_{ce}$ is a function of the activation, $a$, its length, $l_{ce}$, and its contraction velocity $v_{ce}$. These relationships are shown in Figs. 2c and 2d. If the pennation angle $\alpha$ is constant, according to Fig. 2b:

$$l_{mt} = l_{se} + l_{ce}\cos\alpha \tag{4}$$

$$f_{mt} = f_{se} = (f_{ce} + f_{pe})\cos\alpha \approx f_{ce}\cos\alpha \tag{5}$$

where the force of the parallel elastic element PE is set to zero [19–23]. The tendon (SE) can be modeled by a simple quadratic force–strain curve:

$$f_{se} = f_{mt} = \begin{cases} 0 & \text{if } l_{se} < l_{ts} \\ k_t (l_{se} - l_{ts})^2 & \text{if } l_{se} > l_{ts} \end{cases} \tag{6}$$

where $l_{ts}$ is the tendon slack length and $k_t$ is the SE stiffness:

$$k_t = \frac{f_0}{(\varepsilon_0 l_{ts})^2} \tag{7}$$

$\varepsilon_0$ (3% to 5%) is the strain occurring at the maximal isometric muscle force $f_0$, see Winters [24]. The force–length relationship for CE (Fig. 2c) is

$$f_{ce}^* = \frac{f_{ce}}{f_0} = \left[ 1 - \left( \frac{l_{ce} - l_{ce}^{\text{opt}}}{w} \right)^2 \right] \tag{8}$$

where $l_{ce}^{\text{opt}}$ is the muscle fibers optimal length and the width parameter $w$ can be found in [20, 24]. Finally, force-velocity expression for a concentric contraction $v_{ce} < 0$ (Fig. 2d) reads as

$$f_{ce}^* = \frac{f_{ce}}{f_0} = a \cdot \frac{B_r (f_{\text{iso}} + A_r) - A_r \left( B_r - \frac{\dot{l}_{ce}^N}{f_{ac}} \right)}{B_r - \frac{\dot{l}_{ce}^N}{f_{ac}}} \tag{9}$$

where $\dot{l}_{ce}^N = \dot{l}_{ce} / l_{ce}^{\text{opt}}$, $A_r = 0.41$, $B_r = 5.2$, and $f_{\text{iso}} = f_{\text{iso}}(w, l_{ce}^{\text{opt}}, l_{ce})$ is the muscle isometric force relative to the maximal isometric muscle force $f_0$ and $f_{ac} = \min(1, 3.33a)$.

The force–velocity relation, for an eccentric contraction $v_{ce} > 0$ reads as

$$f_{ce}^* = \frac{f_{ce}}{f_0} = a \cdot \frac{b_1 - b_2 (b_3 - \dot{l}_{ce}^N)}{b_3 - \dot{l}_{ce}^N} \tag{10}$$

$$b_2 = -f_{\text{iso}} f_{\text{asymp}} \tag{11}$$

$$b_1 = \frac{f_{ac} B_r (f_{\text{iso}} + b_2)^2}{(f_{\text{iso}} + A_r) \cdot \mathit{slopefactor}} \tag{12}$$

$$b_3 = \frac{b_1}{f_{\text{iso}} + b_2} \tag{13}$$

where $f_{\text{asymp}} = 1.4$ represents the force at infinitely high eccentric velocity and *slopefactor* is the ratio between eccentric and concentric derivatives (i.e., derivative of the muscle CE force with respect to the muscle CE shortening velocity) for an isometric contraction. In this work, we take $\mathit{slopefactor} = 1$ to avoid discontinuities in the objective function, as exposed in [20].

A detailed description of (9)–(13) can be found in [20]. The values for the adopted parameters are shown in Table 1 obtained from [20]. Using (1)–(6) the overall model contraction dynamics equation can be expressed as the nonlinear first-order differential equation (3) [19–23].

### 2.2 Denervated muscles

Injury to the human spinal cord typically results in paralysis of muscles innervated by spinal segments at or below the trauma. Denervated muscles show features of denervation atrophy and weakness [25] whose severity depends on the time elapsed from the injury. Atrophy of

**Table 1** Muscle parameters

| | $l_{ce}^{opt}$ (m) | $w$ | $f_0$ (N) | $l_{ts}$ (m) | $\alpha$ (°) | $l_{m0}$ (m) | $r_a$ (m) | $r_k$ (m) | $r_h$ (m) |
|---|---|---|---|---|---|---|---|---|---|
| Psoas | 0.102 | 1.298 | 821 | 0.142 | 7.5 | 0.248 | 0 | 0 | −0.050 |
| RF | 0.081 | 1.443 | 663 | 0.398 | 5.0 | 0.474 | 0 | 0.050 | −0.034 |
| Glu | 0.200 | 0.625 | 1705 | 0.157 | 3.0 | 0.271 | 0 | 0 | 0.062 |
| BF | 0.104 | 1.197 | 1770 | 0.334 | 7.5 | 0.383 | 0 | −0.034 | 0.072 |
| Vas | 0.093 | 0.627 | 7403 | 0.223 | 4.4 | 0.271 | 0 | 0.043 | 0 |
| Gas | 0.055 | 0.888 | 1639 | 0.420 | 14.3 | 0.404 | 0.053 | −0.020 | 0 |
| TA | 0.082 | 0.442 | 1528 | 0.317 | 6.0 | 0.464 | −0.037 | 0 | 0 |
| Sol | 0.055 | 1.039 | 3883 | 0.245 | 23.6 | 0.201 | 0.053 | 0 | 0 |

these paralyzed muscles is common but the magnitude of the weakness has rarely been evaluated. In [3, 25] the strength of a SCI injured subject's denervated and innervated muscles is reported to vary between 4% and 97% [25].

The AIS (ASIA Impairment Scale) grade indicates the severity of the injury from A (complete) to E (normal motor and sensory functions). In the C and D cases, the motor function is preserved below the neurological level (lowest segment where motor and sensory functions are normal), being the difference between C and D the muscle activity grading.

Nevertheless, the AIS grade has one drawback: muscle scores are poor predictors of intrinsic muscle strength, for example, muscles graded as having normal strength are often considerably weaker than the muscles of able-bodied subjects [25].

On the other hand, the atrophy of denervated muscles increases the passive moments at the inactive joints, which include the moments generated by all other passive structures crossing and surrounding the joints, like ligaments and tissues, also. Several studies [25–28] show that passive torque tended to be larger in the pathological than in the healthy participants, especially at the ankle and hip joints. Nevertheless, the changes in passive stiffness and viscous damping associated to different pathologies seem to be inconsistent [25–28].

In this work, the muscle weakness is modeled limiting the maximum activation of denervated muscles by a weakness factor $p \subset [0, 1]$. The contraction dynamics for a denervated muscle is

$$\dot{f}_{mt} = g\left(l_{mt}, \dot{l}_{mt}, p \cdot a, f_{mt}\right) \tag{14}$$

To model the increment of passive torque due to muscle atrophy, elastic and dissipative elements were added to joints, namely, we used the model developed by Amankwah et al. [28], based upon the Kelvin model for viscoelasticity. In this approach, the Kelvin model was adapted to include a nonlinear elastic element in parallel with both a linear elastic element and a nonlinear viscous element in series. The parameters of the model were estimated from experimental data (isokinetic tests) performed on a sample of both SCI and able-bodied individuals [25–28].

In this work, the nonlinear passive elastic moment was modeled with the traditional double exponential and the parameter values were chosen from [27]. The parameters of the viscoelastic passive moment were taken from [28].

The calculation of the passive torque due to muscle atrophy is important to determine the torque needs of the active orthotic device to assist gait. Figure 3 shows the variation of the ankle, knee and hip moments due to passive torque compared with the reference moments in normal gait (obtained for the benchmark described in Sect. 4). The results show

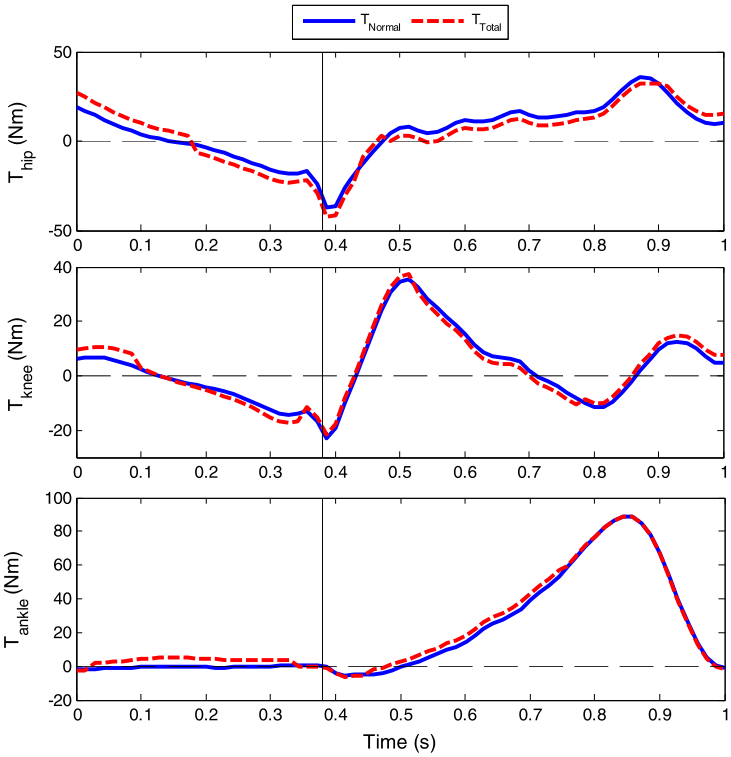


**Fig. 3** Hip, knee, and ankle moments during normal gait (*continuous line*) and variation due to passive torque (*dashed line*)

slight differences except for the hip and knee flexion–extension and ankle dorsiflexion during swing phase (0–0.35 seconds). Assuming that the hip muscles are fully innervated in incomplete SCI subjects, additional passive torque was added to hip joints using parameters for able-bodied subjects [28].

## 3 Optimization approach

Since several muscles serve each joint of the skeletal system, muscle forces cannot be directly computed from joint moments. This is the well-known redundant actuator problem in biomechanics. In order to solve this problem, optimization procedures are used. Several optimization methods (static optimization, dynamic optimization, augmented static optimization, large-scale static optimization) and optimization criteria (minimum metabolical cost of transport, minimum sum of muscle stresses, minimum hyper-extension of the joints, time-integral cost of activations, torque-tracking) are available in the literature [29–43]. The optimization assumes that the load sharing between the muscles follows certain rules during learned motor activities and muscle recruitment strategy is governed by physiologic criteria that achieve functional efficiency. In this work, the muscle-orthosis redundant actuator problem was solved through a physiological static optimization approach.

### 3.1 Static optimization (SO)

The inverse dynamics based static optimization methods are known for 3 decades. In a first step, net joint torques are calculated using the inverse dynamics approach. The muscular load sharing problem is then solved at each time step by minimizing a cost function $J(\mathbf{F}_{mt})$ depending on muscle forces (for example sum of muscle tensions). This optimization problem is subject to the constraint that the sum of muscle moments must equal the net joint torque obtained by inverse dynamics [30].

In the pathological gait of incomplete SCI subjects, the active orthosis should complement the disabled subject's musculoskeletal system so as to provide the efforts required to achieve a motion close to that of normal walking. The load sharing optimization problem for the combined orthosis-SCI subject actuation can be formulated as follows:

$$\begin{aligned} \text{Min} \quad & J(\mathbf{F}_{mt}, \mathbf{T}_o) \\ \text{s.t.} \quad & \mathbf{R} \cdot \mathbf{F} = \mathbf{T} \\ & 0 \le \mathbf{F}_{mt} \le \mathbf{p} \cdot \mathbf{F}_0 \\ & -\mathbf{T}_o^* \le \mathbf{T}_o \le \mathbf{T}_o^* \end{aligned} \tag{15}$$

where $\mathbf{F} = [\mathbf{F}_{mt}, \mathbf{T}_o]^T = [f_{mt,1}, \ldots, f_{mt,N}, T_{o1}, T_{o2}, T_{o3}]^T$ is the muscular and orthosis actuation vector at each instant, $N$ is the number of muscle groups, $\mathbf{R}$ is the constant matrix of equivalent moment arms of the different muscle groups and orthosis actuators and $\mathbf{T}$ is the vector of net joint torques obtained from inverse dynamics analysis considering the dissipative effects of denervated muscles at ankle and knee joints and passive moment at hip joint. Moment arms are defined as the distance between the muscle line of action and the joint axis of rotation. The muscle lengths and moment arms can be determined as functions of the generalized coordinates using expressions or tables available in the literature (see, for example, Menegaldo et al. [35]). The moment arms of each muscle with respect to ankle $r_a$, knee $r_k$, and hip $r_h$ are shown in Table 1.

The second constraint implies that the maximum possible muscular forces are limited by its maximum isometric force $p_i f_{0,i}$, where $\mathbf{F}_0 = [f_{0,1}, \ldots, f_{0,N}]^T$. The third constraint ensures that the orthosis actuation does not exceed the maximum torque available $\mathbf{T}_0^*$.

Two families of cost functions are proposed [8–11]:

$$J_1(\mathbf{F}_{mt}, \mathbf{T}_o) = \omega_{mt} \sum_{j=1}^{N} \left( \frac{f_{mt,j}}{C_j} \right)^n + \omega_o \sum_{k=1}^{3} \left( \frac{T_{o,k}}{T_{o,k}^*} \right)^n \tag{16}$$

$$J_2(\mathbf{F}_{mt}, \mathbf{T}_o) = \omega_{mt} \sum_{j=1}^{N} (-f_{ce,j} v_{ce,j})^n + \omega_o \sum_{k=1}^{3} \left( T_{o,k} \dot{\theta}_k \right)^n \tag{17}$$

where $N$ is the number of muscle groups, $f_{mt,j}$ is the force of muscle unit $j$ and $C_j$ is its physiologic cross-sectional area (PCSA). $T_{o,k}$ is the external torque provided by the orthosis at joint $k$, $\dot{\theta}_k$ is the angular velocity at joint $k$, $n = 2$, and $\omega_{mt}$, $\omega_o$ are the weighting factors assigned to muscular and orthotic actuations, respectively. The first cost function minimizes the weighted sum of muscle stresses raised to the $n$th power and the sum of the orthosis utilization factors at each joint raised to the $n$th power.

The second function minimizes the weighted sum of muscle work rate to the $n$th power and work rate of orthosis actuation.

Static optimization (SO) is computationally efficient compared to dynamic optimization since it does not require multiple integrations of the equations of motion. Nevertheless,

this procedure does not consider the activation and contraction dynamics of the muscle, which can lead to physiological inconsistent results. To overcome this drawback, a simple physiological static optimization approach is proposed in this work.

### 3.2 Physiological static optimization (PSO)

A modified version of the classical static optimization approach that takes into account muscle physiology is proposed in this section. This scheme considers the muscle contraction dynamics, ensuring the physiological consistency of the obtained solution and being efficient from a computational point of view compared to dynamic optimization approaches.

The proposed optimization approach comprises two steps: in the first step, the inverse contraction dynamics problem is solved, assuming that muscle activations are maxima. The second step calculates the activations compatible with the net joint torques obtained by inverse dynamics using a static optimization approach.

In the first step, the length and velocity of each musculotendon unit $l_{mt}, \dot{l}_{mt}$ are obtained from generalized coordinates of the multibody model and the initial musculotendon lengths $l_{m0}$ (Table 1). Then, the maximum muscle force histories $f^*_{mt}(t)$ compatible with contraction dynamics are calculated supposing that the muscle activation are maxima at every instant $\mathbf{A}_m = [a_1, \ldots, a_N]^T = [1, \ldots, 1]^T$. The initial condition to obtain the maximum muscle force histories is determined by assuming $F_m(t=0) = k_t \cdot (l_{se} - l_{\text{slack}})^2$ where $l_{se} = l_{se}(l_m, l_{ce})$ and $l_{ce}(t=0) = l_m - l_{\text{slack}}$.

Briefly, for each muscle, the contraction dynamics differential equation is integrated:

$$\frac{df^*_{mt}}{dt} = g\big((a=1)\cdot p, f^*_{mt}, l_{mt}, \dot{l}_{mt}\big) \tag{18}$$

In the second step, the muscle activations and orthosis actuation is calculated solving the optimization problem:

$$\begin{aligned} \text{Min} \quad & J_1(\mathbf{A}_m, \mathbf{A}_o) = \omega_{mt} \sum_{j=1}^{N} \left( \frac{a_j f^*_{mt,j}}{C_j} \right)^2 + \omega_o \sum_{k=1}^{3} \left( \frac{o_k T^*_{o,k}}{T^*_{o,k}} \right)^2 \\ \text{s.t.} \quad & \mathbf{R} \cdot (\mathbf{AF}^*) = \mathbf{T} \\ & 0 \le a_j \le 1 \\ & -1 \le o_k \le 1 \end{aligned} \tag{19}$$

where $\mathbf{AF}^*_{mt} = [a_1 \cdot p_1 \cdot f^*_{mt,1}, \ldots, a_N \cdot p_N \cdot f^*_{mt,N}, o_1 \cdot T^*_{o,1}, o_2 \cdot T^*_{o,2}, o_3 \cdot T^*_{o,3}]^T$. The variables $o_k$ ensure that the orthosis actuation does not exceed the maximum available actuator torque at joint $k$. The cost function in (19) is not dimensionally consistent, so $\omega_o$ must be chosen in order to balance the weights of muscle stresses and orthosis actuation. This balance, in terms of weights reads as:

$$\omega_{mt} \sum_{j=1}^{N} \left( \frac{a_j f^*_{mt,j}}{C_j} \right)^2 \approx \omega_o \sum_{k=1}^{3} \left( \frac{o_k T^*_{o,k}}{T^*_{o,k}} \right)^2$$

The maximum value for this expression will be achieved for $a_j = 1$ for $j = 1, \ldots, 8$ and $o_k = 1$ for $k = 1, 2, 3$. In this way, if the value of $\omega_{mt}$ is chosen as $\omega_{mt} = 1$, and $C_j = PCSA_j = \frac{F_{\max,j}}{\sigma_j}$, where $\sigma_j = 0.25 \cdot 10^6$ for all the muscles for the sake of simplicity, then the following value for $\omega_0$ can be easily obtained as

$$\omega_0 \approx \omega_{mt} \frac{\sum_{j=1}^{8} \frac{F_{\max,j}}{F_{\max,j}/\sigma_j}}{\sum_{k=1}^{3} o_k} \approx 5.55 \cdot 10^{10}$$

In order to compare the results of static and physiological static optimization, the function:

$$J_2(\mathbf{F}_{mt}, \mathbf{T}_o) = \omega_{mt} \sum_{j=1}^{N} (-f_{ce,j} v_{ce,j})^n + \omega_o \sum_{k=1}^{3} \left(T_{o,k} \dot{\theta}_k\right)^n \tag{20}$$

was also minimized using the physiological static optimization approach.

This procedure generates activation patterns consistent with contraction dynamics only if muscle force ($f_{mt}$) scales linearly with muscle activation. This is certainly not the case for standard Hill-models. Nonetheless activations obtained via the physiological static optimization approach were introduced in the contraction dynamics to compare the muscular forces achieved with this process, and they yielded a very accurate result thus ensuring its physiological consistency.

## 4 Results and discussion

The static and physiological static approaches ((15)–(17) and (19)–(20), respectively) were applied to calculate muscle forces and orthosis actuation during walking in order to assist the pathological gait. In the adopted procedure, normal gait motion data is used as input to the biomechanical model. Namely, the 2D walking kinematic Benchmark data from Winter [38] was used to perform an inverse dynamic analysis. The acquired movement is a normal cadence nonpathological gait stride, carried out by a healthy female subject with 57.75 kg of weight. The analysis comprises a period of 1 s. The kinematic data was acquired using a sampling frequency of 70 Hz. The obtained net driver ankle and knee moments were corrected to consider the dissipative effects of muscle atrophy in SCI subjects (Fig. 3).

The optimization problems were solved using the MATLAB™ gradient-based routine "fmincon" implemented in the Optimization Toolbox that uses a sequential quadratic programming (SQP) method. Two different sets of innervated muscles were compared in order to compare the results for an AIS C and AIS D SCI subject. According to ASIA Impairment Scale:

- AIS C: Motor function is preserved below the neurological level, and more than half of key muscles below the neurological level have a muscle grade less than 3. In this case, the innervated and denervated muscles were defined by the vector $\mathbf{p} = [1, 0.2, 1, 0.2, 0.2, 0.2, 0.2, 0.2]^T$. See Fig. 1b for muscle description.
- AIS D: Motor function is preserved below the neurological level, and at least half of key muscles below the neurological level have a muscle grade of 3 or more. In this case, the innervated and denervated muscles were represented by the vector $\mathbf{p} = [1, 1, 1, 1, 0.4, 0.4, 0.4, 0.4]^T$.

Figures 4, 5, and 6 represent the muscle and orthosis actuation obtained using the static and physiological static approaches for AIS C and AIS D subjects.

The results using static and physiological static optimization were similar, according to results obtained by other authors [32] due to low contraction velocities for gait, except for the Soleus and Tibialis anterior muscles. The weighting factors for cost function $J_1$ were $\omega_{mt} = 1$ and $\omega_o = 5.5 \cdot 10^{10}$ (to balance the weights of muscle stresses and orthosis actuation) and for cost function $J_2$ were $\omega_{mt} = 1$ and $\omega_o = 1$. Results show that a proper designed HKAFO can assist the pathological gait cycle of both AIS C and D incomplete SCI subjects to approach normal kinetic gait patterns at joints.

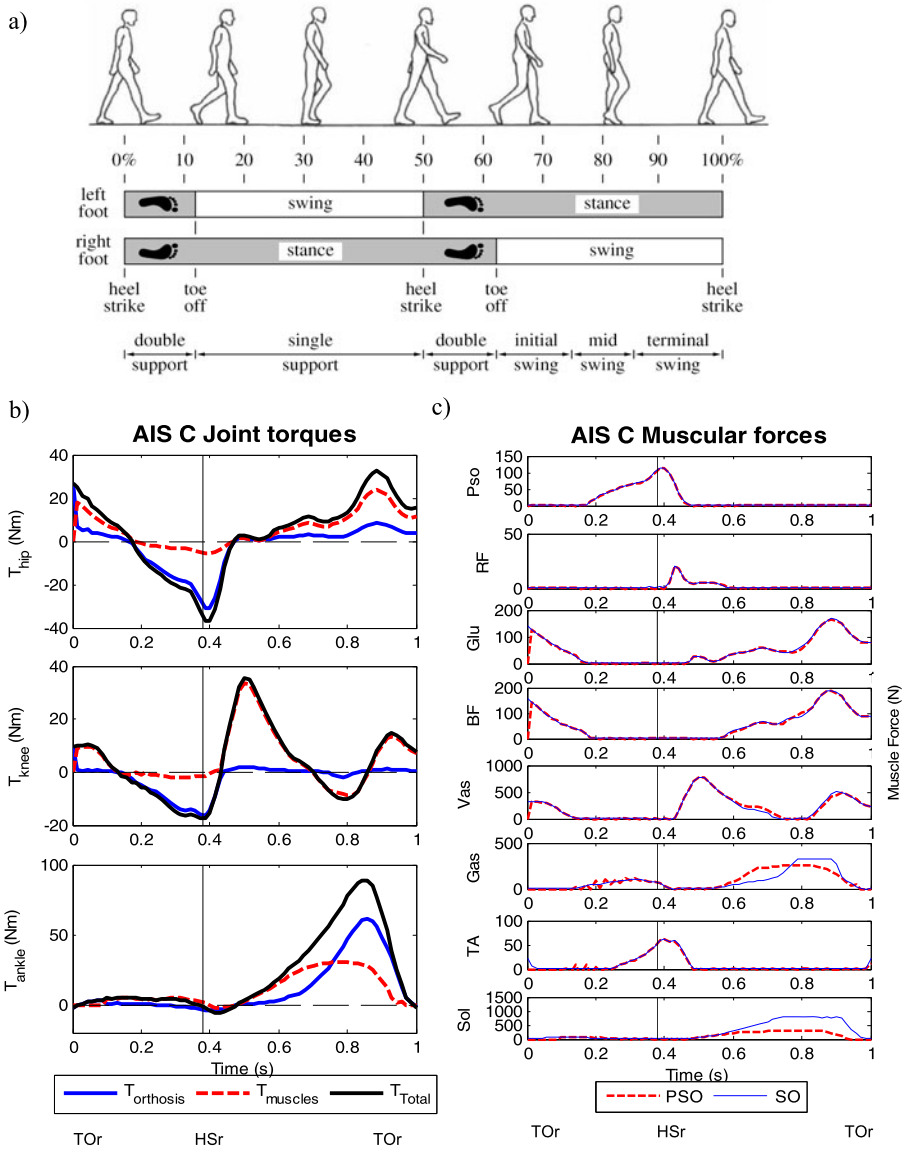


**Fig. 4** Results (**a**) Human gait phases. Source: [19], (**b**) Joint torques for an ASIA C subject obtained by PSO and using cost function $J_1$, and (**c**) Muscular forces for an ASIA C subject obtained by SO and PSO and using cost function $J_1$. TOr, right toe off.; HSr, right heel strike. *Vertical continuous line* separates swing and stance phases

The orthosis actuation prevents stance phase knee flexion due to quadriceps weakness, assists swing-phase knee flexion-extension and corrects insufficient ankle plantarflexor torque to achieve normal moment patterns at the hip, knee, and ankle joints during gait.

Figures 4, 5 and 6 reveal that the torque needs of the active orthotic device are similar to the ones developed by the human ankle, knee, and hip joints. The calculated maximum

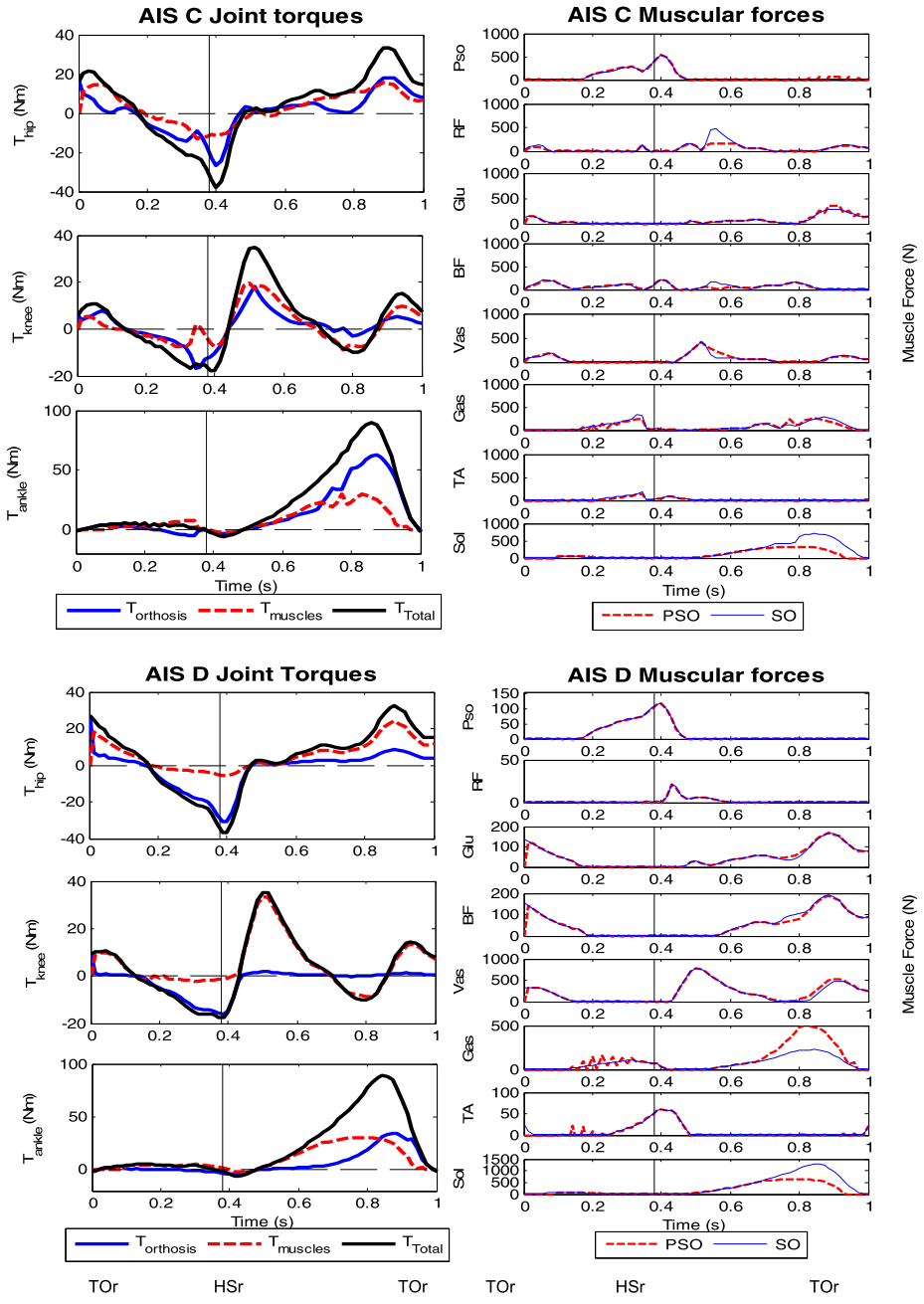


**Fig. 5** (**a**) Joint torques for an ASIA C subject obtained by PSO and using cost function $J_2$, (**b**) Muscular forces for an ASIA C subject obtained by SO and PSO and using cost function $J_2$, (**c**) Joint torques for an ASIA D subject obtained by PSO and using cost function $J_1$, and (**d**) Muscular forces for an ASIA D subject obtained by SO and PSO and using cost function $J_1$. TOr, right toe off.; HSr, right heel strike

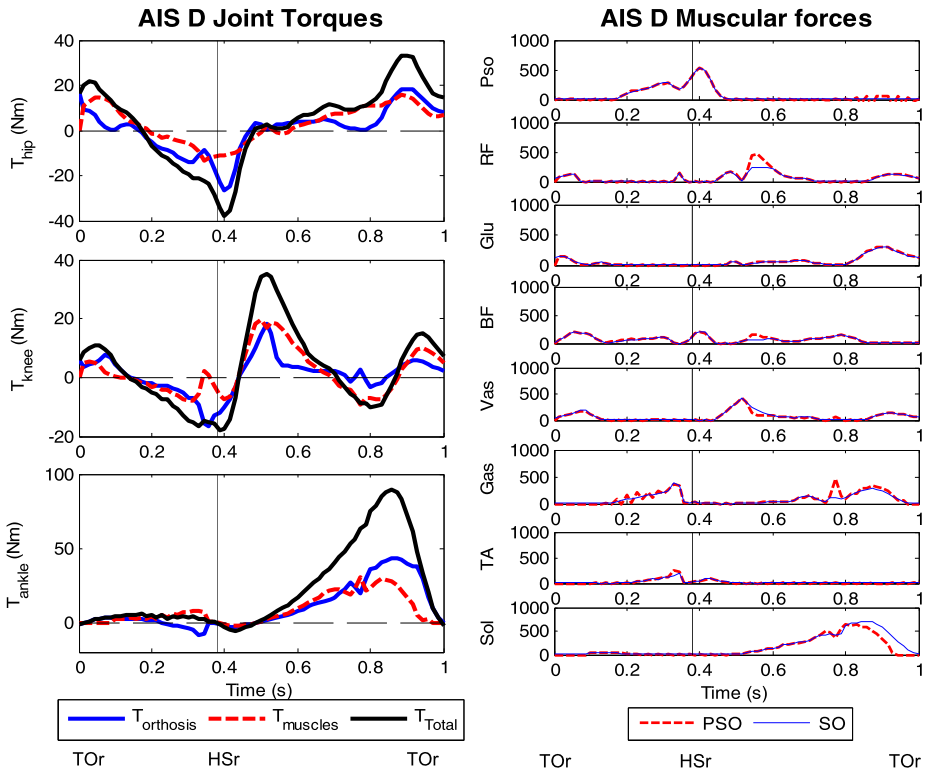


**Fig. 6** (**a**) Joint torques for an ASIA D subject obtained by PSO and using cost function $J_2$, (**b**) Muscular forces for an ASIA D subject obtained by SO and PSO and using cost function $J_2$. TOr, right toe off.; HSr, right heel strike

required torque for the orthosis is about 30 N m at the hip and 20 N m at the knee for both AIS C subjects and AIS D subjects. During stance phase, the orthosis modulates the plantarflexor torque according to injury severity AIS C or AIS D. The needed external actuation at the ankle is 65 N m for AIS C subjects and about 40 N m for AIS D subjects. The obtained powered assistances at the ankle and at the hip were comparable to those obtained using an EMG-driven ankle exoskeleton and a foot switch based control hip exoskeleton respectively [2–4]. Namely, in [3] the peak plantar flexion torque provided by the ankle exoskeleton was ($50 \pm 12$ N m) and in [4] the hip exoskeleton provides approximately 23 N m of hip flexion torque during the initial stance phase.

Note that the obtained results must be interpreted with caution, since the muscle weakness coefficient $p$ must be evaluated in real SCI subjects. Moreover, the weight of the orthosis has been neglected and this mass would increase the required moments at the hip and knee joints, especially at the hip and knee during the swing phase as reported by other authors [1].

Regarding the computational cost of each formulation, the CPU mean time was 10.29 s for the static optimization approach. To solve the physiologic static optimization problem, first, the contraction equation (18) was integrated using the Euler method (CPU time 0.42 s) and the optimization problems (19) and (20) were solved in a mean time of 9.04 s. The initial guess for the two approaches (SO and PSO) was zero. The results show that the

computational cost of the proposed approach is low compared with other physiological static formulations proposed [20–23, 35].

## 5 Conclusions

This work presents a simple and efficient approach to estimate muscle forces and orthosis actuation in powered assisted walking of incomplete spinal cord-injured subjects. Using moment pattern data of normal gait helps in the definition of the actuation for the design of the active orthosis prototype. In fact, several studies [44, 45] use normal joint torque data to determine the actuation to be applied at each assisted joint. Nevertheless, one of the major challenges in exoskeleton research is the understanding of the underlying mechanisms that are responsible for control in both able-bodied and disabled subjects and, in particular, how those interact with a robotic device in parallel with the wearer. There are few papers which test and demonstrate that able bodied subjects reduce net muscle moments about their joints when robotic assistance is provided [46–48]. On the contrary, no studies have been published characterizing the combined human-orthosis actuation of active orthoses developed specifically for use with SCI individuals. In this context, extensive experimental research in this topic, including training of SCI subjects in orthosis usage, is necessary to test the validity of the invariant moment hypothesis and to adapt the weighting factors in the objective function (and) to the real SCI-orthosis system behavior. The proposed scheme is computationally efficient and ensures the physiological consistency of the obtained results. The major contribution of the optimization approach is that the contraction dynamics equation is integrated in a first step to obtain the maximum physiologic available muscle forces. The final objective is to develop a computer application that enables to virtually test different types of active orthoses for gait assistance on disabled subjects suffering from spinal cord injury and other gait pathologies. The results of this application are the efforts of the disabled subject, along with the orthosis forces required to produce the desired normal kinetic gait patterns at joints. The obtained results seem to be promising, nevertheless to attain the final objective much work has to be done in several topics:

- Include in the optimization problem the contact loads transmitted at the leg-orthosis interface in order to obtain contact pressures below the PPTs (Pain Pressure Thresholds), which represent the patient's comfort.
- The optimization cost function adopted for disabled-bodied subjects will be revised since disability may affect it. Moreover, in future works, the activation dynamics will be taken into account to obtain the metabolic cost of transport.
- The way in which the disability affects the subject will have to be deeply investigated in order to make the corresponding changes in the model of able-bodied subject so as to obtain a model of disabled subject. Namely, the force-generation dynamics and the parameters of the impaired muscle and passive torque due to muscle atrophy will be adapted according to the results available in the literature for the considered disability. Such a model will undergo then a validation procedure.
- The obtained results must be compared with forward dynamics optimization and parametric schemes. To test the hypothesis of net joint moment invariance, the forward dynamics module should determine the kinematics, along with the combined actuation of the musculoskeletal system and the active orthosis. In this case, the desired motion of the disabled subject wearing the active orthosis is no longer available, so, a scaled-normalized able-bodied gait pattern, consistent with the anthropometric dimensions of the disabled subject, should be first defined to evaluate the quality of the obtained solution.

- A walking aid mimicking canes and voluntary upper extremity actions to maintain lateral stability by providing the necessary shoulder forces and moments must be included in the inverse or forward dynamic simulations in order to obtain more realistic results.

**Acknowledgement** This work is supported by the Spanish Ministry of Science and Innovation under the project DPI2009-13438-C03. The support is gratefully acknowledged.

## References

1. Silva, P.C., Silva, M.T., Martins, J.M.: Evaluation of the contact forces developed in the lower limb/orthosis interface for comfort design. Multibody Syst. Dyn. **24**, 367–388 (2010)
2. Kao, P.C., Lewis, C.L., Ferris, D.P.: Invariant ankle moment patterns when walking with and without a robotic ankle exoskeleton. J. Biomech. **43**, 203–209 (2010)
3. Kao, P.C., Lewis, C.L., Ferris, D.P.: Joint kinetic response during unexpectedly reduced plantar flexor torque provided by a robotic ankle exoskeleton during walking. J. Biomech. **43**, 1401–1407 (2010)
4. Lewis, C.L., Ferris, D.P.: Invariant hip moment pattern while walking with a robotic hip exoskeleton. J. Biomech. **44**, 789–793 (2011)
5. Pons, J.L.: Wearable Robots: Biomechatronic Exoskeletons. Wiley/Blackwell, New York (2008)
6. To, C.S., Kirsch, R.F., Kobetic, R., Triolo, R.J.: Simulation of a functional neuromuscular stimulation powered mechanical gait orthosis with coordinated joint locking. IEEE Trans. Neural Syst. Rehabil. Eng. **13**(2), 227–235 (2005)
7. Agrawal, S.K., Fattah, A.: Theory and design of an orthotic device for full or partial gravity-balancing of a human leg during motion. IEEE Trans. Neural Syst. Rehabil. Eng. **12**(2), 157–165 (2004)
8. Vukobratovic, M., Ciric, V., Hristic, D.: Contribution to the study of active exoskeletons. In: Proceedings of the 5th IFAC Congress. Paris, France (1972)
9. Vukobratovic, M., Hristic, D., Stojiljkovic, Z.: Development of active anthropomorphic exoskeleton. Med. Biol. Eng. Comput. **12**, 66–80 (1974)
10. Dollar, A.M., Herr, H.: Active orthoses for the lower-limbs: challenges and state of the art. In: Proceedings of the 2007 IEEE 10th International Conference on Rehabilitation Robotics, pp. 968–977. Noordwijk, The Netherlands (2007)
11. Colombo, G., Jorg, M., Dietz, V.: Driven gait orthosis to do locomotor training of paraplegic patients. In: 22nd Annual International Conference of the IEEE-EMBS. Chicago, USA (2000)
12. Pratt, J., Krupp, B., Morse, C., Collins, S.: The roboKnee: an exoskeleton for enhancing strength and endurance during walking. In: IEEE Int. Conference on Robotics and Automation. New Orleans, USA (2004)
13. Kawamoto, H., Kanbe, S., Sankai, Y.: Power assist method for HAL-3 estimating operator's intention based on motion information. In: Proceedings of 2003 IEEE Workshop on Robot and Human Interactive Communication, pp. 67–72. Millbrae, CA, IEEE, New York (2003)
14. Kawamoto, H., Sankai, Y.: Power assist system HAL-3 for gait disorder person. In: ICCHP. Austria (2002)
15. Blaya, J.A., Herr, H.: Adaptive control of a variable-impedance ankle-foot orthosis to assist drop-foot gait. IEEE Trans. Neural Syst. Rehabil. Eng. **12**, 24–31 (2004)
16. Yamaguchi, G.T., Zajac, F.E.: Restoring unassited natural gait to paraplegics via functional neuromuscular stimulation: a computer simulation study. IEEE Transactions on Biomedical Engineering **37**(9) (1990)
17. Zajac, F.: Muscle and tendon: properties, models, scaling and applications to biomechanics and motor control. Crit. Rev. Biomed. Eng. **17**, 359–411 (1989)
18. Hill, A.: The heat of shortening and the dynamic constants of muscle. Proc. R. Soc. Lond. B, Biol. Sci. **126**, 136–195 (1938)
19. Ackermann, M., Schiehlen, W.: Dynamic analysis of human gait disorder and metabolical cost estimation. Arch. Appl. Mech. **75**, 569–594 (2006)
20. Ackermann, M.: Dynamics and energetics of walking with prostheses. Ph.D. thesis, University of Stuttgart, Stuttgart (2007)
21. Rodrigo, S.E., Ambrósio, J.A.C., Silva, M.P.T., Penisi, O.H.: Analysis of human gait based on multibody formulations and optimization tools. Mech. Based Des. Struct. Mach. **36**, 446–477 (2008)
22. García, D., Schiehlen, W.: Simulation of human walking with one-sided gait. In: Proceedings of the 1st Joint International Conference on Multibody System Dynamics. 1st Joint International Conference on Multibody System Dynamics (1). Num. 1. Lapperanta, Finland (2010)

23. Winters, J.: Concepts in Neuromuscular Modeling, Three-dimensional Analysis of Human Movement. Human Kinetics Publishers, Champaign (1995)
24. Thomas, C.K., Grumbles, R.M.: Muscle atrophy after human spinal cord injury. Biocybern. Biomed. Eng. **25**(3), 39–46 (2005)
25. McDonald, M.F., Garrison, M.K., Schmit, B.D.: Length–tension properties of ankle muscles in chronic human spinal cord injury. J. Biomech. **38**, 2344–2353 (2005)
26. Lebiedowska, M.K., Fisk, J.R.: Passive dynamics of the knee joint in healthy children and children affected by spastic paresis. Clin. Biomech. **14**(9), 653–660 (1999)
27. Edrich, T., Riener, R., Quintern, J.: Analysis of passive elastic joint moments in paraplegics. IEEE Trans. Biomed. Eng. **47**, 1058–1065 (2000)
28. Amankwah, K.R., Triolo, J., Kirsch, R.: Effects of spinal cord injury on lower-limb passive joint moments revealed through a nonlinear viscoelastic model. J. Rehabil. Res. Dev. **41**, 15–32 (2004)
29. Nigg, B.M., Herzog, W. (eds.): Biomechanics of the Musculo-Skeletal System, 2nd edn. Wiley, New York (1999)
30. Crowninshield, R., Brand, R.A.: A physiologically based criterion of muscle force prediction in locomotion. J. Biomech. **14**, 793–801 (1981)
31. Yamaguchi, G.T., Moran, D.W., Si, J.: A computationally efficient method for solving the redundant problem in biomechanics. J. Biomech. **28**, 999–1005 (1995)
32. Anderson, F.C., Pandy, M.G.: Static and dynamic optimization solutions for gait are practically equivalent. J. Biomech. **34**, 153–161 (2001)
33. Rengifo, C., Aoustin, Y., Plestan, F., Chevallereu, C.: Distribution of forces between synergistics and antogonistics muscles using an optimization criterion depending on muscle contraction behaviour. J. Biomech. Eng. **132**, 1–11 (2010)
34. Anderson, F.C., Pandy, M.G.: Dynamic optimization of human walking. J. Biomech. Eng. **123**, 381–390 (2001)
35. Menegaldo, L.L., Fleury, A.T., Weber, H.I.: A 'cheap' optimal control approach to estimate muscles forces in musculoskeletal systems. J. Biomech. **39**, 1787–1795 (2006)
36. Thelen, D.G., Anderson, F.C.: Using computed muscle control to generate forward dynamic simulations of human walking from experimental data. J. Biomech. **39**, 321–328 (2006)
37. Pipeleers, G., Demeulenaere, B., Jonkers, I., Spaepen, P., Van der Perre, G., Spaepen, A., Swevers, J., De Schutter, J.: Dynamic simulation of human motion: numerically efficient inclusion of muscle physiology by convex optimization. Optimization. Engineering **9**, 213–238 (2008)
38. Winter, D.A.: Biomechanics and Motor Control of Human Gait: Normal, Elderly and Pathological, 2nd edn. University of Waterloo Press, Waterloo (1991)
39. Ambrosio, J., Kecskemethy, A.: Multibody dynamics of biomechanical models for human motion via optimization. In: Garcia Orden, J.C., Goicolea, J.M., Cuadrado, J. (eds.), Multibody Dynamics Computational Methods and Applications. Springer, Berlin (2007)
40. Tsirakos, D., Baltzopoulos, V., Barlett, R.: Inverse optimization: functional and physiological considerations related to the force-sharing problem. Crit. Rev. Biomed. Eng. **25**, 371–407 (1997)
41. Hatze, H.: Neuromusculoskeletal control systems modeling: a critical survey of recent developments. IEEE Trans. Autom. Control **25**, 375–385 (1980)
42. Ralston, H.J.: Energetics of Human Walking, Neural Control of Locomotion. Plenum, New York (1976)
43. Hatze, H.: The fundamental problem of myoskeletal inverse dynamics and its implications. J. Biomech. **35**, 109–115 (2002)
44. Au, S., Berniker, M., Herr, H.: Powered ankle-foot prosthesis to assist level-ground and stair-descent gaits. Neural Netw. **21**(4), 654–666 (2008)
45. Cullell, A., Moreno, J.C., Rocon, E., Forner-Cordero, A., Pons, J.L.: Biologically based design of an actuator system for a knee-ankle-foot orthosis.. Mech. Mach. Theory **44**, 860–872 (2009)
46. Kao, P.-C., Ferris, D.P.: Motor adaptation during dorsiflexion-assisted walking with a powered orthosis. Gait Posture **29**(2), 230–236 (2009)
47. Cain, S.M., Gordon, K.E., Ferris, D.P.: Locomotor adaptation to a powered ankle-foot orthosis depends on control method. J. NeuroEng. Rehabil. **4**, 48 (2007)
48. Ferris, D.P., Bohra, Z.A., Lukos, J.R., Kinnaird, C.R.: Neuromechanical adaptation to hopping with an elastic ankle-foot orthosis. J. Appl. Physiol. **100**(1), 163–170 (2006)